

## Valence Band Photoemission Study of the Kondo Insulator CeNiSn

J. -S. Kang

*Department of Physics, The Catholic University of Korea, Puchon 422-743, Korea*

C. G. Olson

*Ames Laboratory, Iowa State University, Ames, Iowa 50011, U. S. A.*

Y. Ōnuki

*Faculty of Science, Osaka University, Toyonaka, Osaka 560, Japan, and  
Advanced Science Research Center, Japan Atomic Energy Research Institute,  
Tokai, Ibaraki 319-11, Japan*

(Received 4 September 1997)

The electronic structure of the Kondo insulator CeNiSn has been investigated by using photoemission spectroscopy. A satellite feature is observed in the valence band spectrum about 6 eV below the Ni 3*d* main peak, indicating a strong Ni 3*d* Coulomb correlation in CeNiSn. The Ce 4*f* partial spectral weight exhibits three peak structures, including one due to the 4*f*<sup>1</sup> → 4*f*<sup>0</sup> transition, another near E<sub>F</sub>, and the other which overlaps the Ni 3*d* main peak. We interpret the peak near E<sub>F</sub> as reflecting mainly the Ce 4*f*/Sn 5*p* hybridization, whereas that around the Ni 3*d* main peak as reflecting both the Ce 4*f*/Ni 3*d* and Ce 5*d*/Ni 3*d* hybridization. Yield measurements across the 4*d* → 4*f* threshold indicate the Ce valence to be close to 3+. The prominent Fermi edge suggests a metallic ground state in CeNiSn.

### 1. Introduction

CeNiSn is considered to be a valence-fluctuating compound with an anomalous ground state [1-5]. CeNiSn is classified as a Kondo insulator since transport and magnetic measurements on CeNiSn indicate the energy gap formation in the non-magnetic ground state below T<sub>g</sub> ≈ 6 K (T<sub>g</sub>: the gap formation temperature). The characteristic Kondo temperature T<sub>K</sub> is estimated to be 40-80 K [6]. In addition, temperature(T)-dependent gap developments and an anisotropic energy gap were observed in the tunneling spectroscopy measurements [7]. The estimated energy gap (10 K) [2, 7] is an order of magnitude smaller than those of valence-fluctuating Sm and Yb compounds [8]. Therefore, much interest has been focused on how such a small energy gap is caused by strong correlations in the Kondo lattice.

Despite extensive studies on CeNiSn, there are several unresolved issues. First, the origin of the energy gap formation is not understood yet. This gap is considered to be formed within the narrow Ce 4*f* states, but there has been no commonly accepted explanation [9, 10]. CeNiSn does not order

magnetically [11], but there is an evidence of the existence of a quasi-one dimensional anti-ferromagnetic correlation [12]. The role of anti-ferromagnetic spin fluctuations on the energy gap formation has not been fully understood. Secondly, a question on the intrinsic ground state of CeNiSn has been recently raised, because of the finding of the metallic-like T-dependent electrical resistivity in a purified single crystal of CeNiSn [5, 13]. This work has brought on a controversy between the metallic and insulating intrinsic ground state of CeNiSn, and also suggested the importance of experiments on high quality single crystals.

To resolve the above issues on CeNiSn, it is important to investigate its electronic structure. Band structure calculations predict CeNiSn to be a semi-metal or a small-gap insulator with an anisotropic hybridization gap state [14, 15]. Only a few experimental studies have been reported on its electronic structure. Based on valence band and core level photoemission spectroscopy (PES) measurements on polycrystalline CeTSn (T = Ni, Pd, Pt) [16], it has been argued that the valence of Ce is close to trivalent and that the Ce 4*f* states are strongly hybridized with the Sn 5*p* states in CeNiSn.

In this paper we report valence band PES measurements on a high quality single crystalline CeNiSn. We have also performed yield measurements near the Ce 4d absorption edge to determine the bulk Ce valence more accurately.

## 2. Experimental Details

Single crystals of CeNiSn were grown by the Czochralski pulling method by using a tungsten crucible in an rf furnace. The ingot sample was purified by the technique of solid-state electro-transport [5]. Photoemission experiments were carried out at the Ames/Montana ERG/Seya beamline at the Synchrotron Radiation Center. The samples were cleaved in vacuum with a base pressure better than  $4 \times 10^{-11}$  Torr. Temperature was controlled by placing the samples in direct contact with a cryostat cooled down to 20 K using a closed cycle He refrigerator. The Fermi level  $E_F$  and the overall instrumental resolution of the system were determined from the valence band spectrum of a sputtered Pt foil near  $E_F$ . The total instrumental resolution [FWHM:full width at half maximum] was about 150 meV at  $h\nu = 20\text{-}70$  eV and 250 meV at  $h\nu \approx 120$  eV. The photon flux was monitored by the yield from a gold mesh and all the spectra reported are normalized to the mesh current.

## 3. Results and Discussion

Figure 1 shows the valence band energy distribution curves (EDCs) of CeNiSn in the photon energy  $h\nu$  range of 14-121 eV, including both the Ni 3p and Ce 4d absorption thresholds ( $\sim 68$  eV and  $\sim 120$  eV, respectively). As  $h\nu$  varies, the line shape of the valence band spectrum changes, which is mainly due to the change in the relative photoionization cross sections of different electronic states [17].  $h\nu = 121$  eV and  $h\nu = 115$  eV correspond to the on- and off-resonance energies, respectively, corresponding to the Ce 4d  $\rightarrow$  4f absorption [18]. Therefore the emission between  $E_F$  and about 3 eV in binding energy (BE) which is enhanced at  $h\nu = 121$  eV is identified with the Ce 4f emission, whereas the off-resonance spectrum at  $h\nu = 115$  eV is dominated by the Ni 3d emission. The line shape does not change from  $h\nu \approx 115$  eV down to  $h\nu = 63$  eV, indicating that Ni 3d emissions dominate in this photon energy range.  $h\nu = 68$  eV and  $h\nu = 63$  eV correspond to the Ni 3p  $\rightarrow$  3d on- and off-resonance energies, respectively. At  $h\nu = 68$  eV, the main peak around 1.4 eV in BE and the satellite peak around 6 eV below the main peak can be roughly assigned to the  $3d^9 c^{m-1}$  and  $3d^8 c^m$  final state configurations, respectively, as in pure Ni metal (c: conduction or ligand electrons) [19]. The satellite structure associated with the Ni 3d bands is not explained by one electron band theory, and it is taken to arise from the Ni 3d Coulomb correlation. At low  $h\nu$ 's (14-30 eV), besides the Ni 3d main peak at 1.4 eV in BE, three other weak structures are observed at  $E_F$ ,  $\sim 0.8$  eV, and  $\sim 2.2$  eV in BE, which diminish with increasing  $h\nu$ . Since the Sn 5p and Ce 5d cross sections become larger with re-

spect to that of the Ni 3d electrons at these lower  $h\nu$ 's than at higher  $h\nu$ 's, these three weak structures seem to have the Sn 5p and Ce 5d characters. This conclusion implies that the Sn 5p and Ce 5d states in CeNiSn are spread over the whole valence band, i.e., from  $E_F$  to  $\sim 4$  eV below.

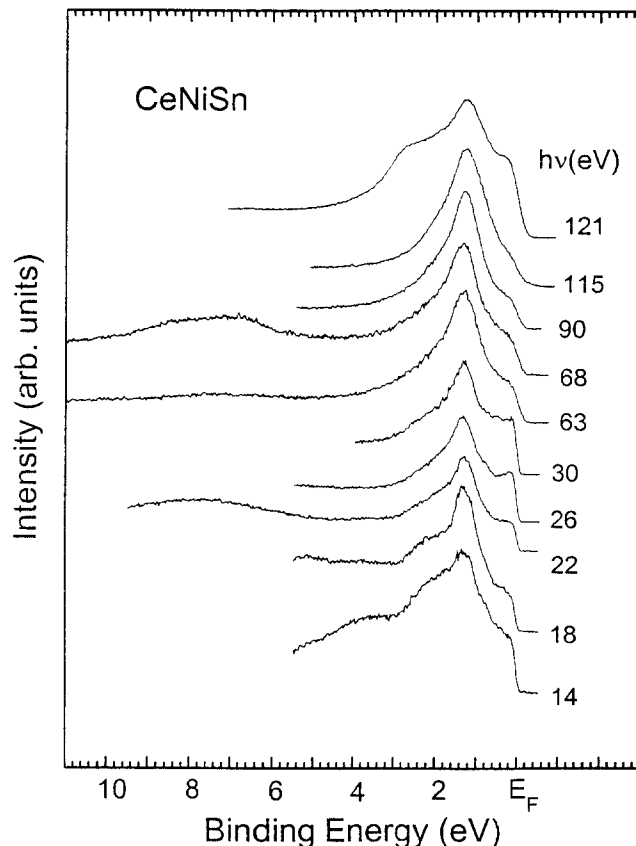


Fig. 1. Valence band photoemission spectra of CeNiSn over a wide photon energy  $h\nu$  range.

A shoulder-like structure is observed near  $E_F$  in all the spectra for  $h\nu$ 's in 14-121 eV. Such a structure has not been observed in Ref. [16], which reflects a better energy resolution and a better quality of the sample employed in this study. The intensity at  $E_F$  relative to that of the Ni 3d main peak (1.4 eV in BE) remains essentially the same from  $h\nu \sim 60$  eV to  $h\nu = 115$  eV, indicating the presence of Ni 3d states near  $E_F$ . In contrast, the intensity close to  $E_F$  becomes enhanced at  $h\nu \approx 26$  eV, suggesting the presence of the Sn 5p and Ce 5d states [17]. Besides these electronic states, there are also the Ce 4f states near  $E_F$ , which will be shown in Fig. 2. Thus the Fermi edge in CeNiSn seems to have a mixed character, i.e., a mixture of the Sn 5p/Ce 5d, Ce 4f, and Ni 3d characters. This interpretation is consistent with the theoretical prediction [15, 20].

Figure 2 presents the extracted Ce 4f partial spectral weight (PSW) distribution (dots), and the subtraction procedure of the Ce 4d  $\rightarrow$  4f off-resonance spectrum (dashed line) from the on-resonance spectrum (solid line). The  $h\nu = 115$  eV spectrum has

been scaled by a factor  $\alpha=0.93$  to account for the  $h\nu$  dependence of the Ni  $3d$  cross section [17]. The difference curve exhibits three prominent features at about 0.3 eV ("A"), 1.4 eV ("B") in BE, and 2.7 eV ("C") in BE. It is still necessary to separate out the Ce  $4f$  bulk emission from the Ce  $5d$  emission. The Ce  $5d$  emission is known to resonate at the  $4d$  absorption edge as well [21], and so at least some portion of the difference curve (dots) should be identified with the Ce  $5d$  emission. As will be discussed later, a substantial contribution from the Ce  $5d$  PSW lies under the structure "B".

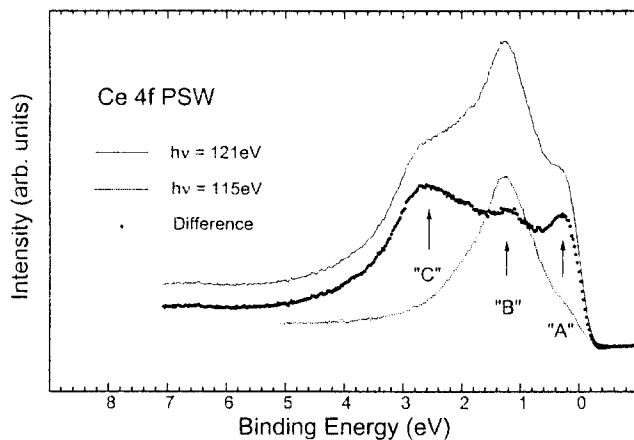


Fig. 2. The extracted Ce  $4f$  spectrum (dots) of CeNiSn. The subtraction of the Ce  $4d \rightarrow 4f$  off-resonance spectrum (dashed line) from the on-resonance spectrum (solid line) is also shown.

The peaks "A" and "C" are reminiscent of the well-known double-peak structures observed in Ce metal and Ce compounds. The peak "C" corresponds to the  $4f^1 \rightarrow 4f^0$  transition [22]. The  $4f$  spectral intensity close to  $E_F$  ("A") is known to reflect the strength of the hybridization between Ce  $4f$  and conduction band electrons, corresponding to the  $4f^1 c^{m-1}$  final state [18, 23-25]. In terms of the Gunnarsson/Schönhammer (G/S) theory [23], based on the degenerate impurity Anderson Hamiltonian (IAH) assuming Ce  $4f$  electrons to be essentially localized, the spectral feature "A" close to  $E_F$  corresponds to the tail of the Kondo resonance and it originates from the hybridization interaction between Ce  $4f$  and conduction band electrons and the on-site Coulomb interaction between Ce  $4f$  electrons. In the band theoretical view, the peak near  $E_F$  is interpreted as the ground state Ce  $4f$  band, corresponding to the fully relaxed  $4f^1 c^{m-1}$  final states [24].

Even though the detailed origin of the near  $E_F$  peak is still controversial, the substantially large intensity of the peak "A" suggests large hybridization, as discussed below. The average separation between Ce sites in CeNiSn ( $d = 3.82$  Å) is larger than the Hill limit (3.3-3.5 Å), corresponding to the local moment formation, and even larger than that in  $\gamma$ -Ce and  $\alpha$ -Ce ( $d(\gamma\text{-Ce}) = 3.65$  Å and  $d(\alpha\text{-Ce}) = 3.39$  Å), suggesting the direct interaction between near neighbor Ce  $4f$  electrons to be negligible in CeNiSn. Thus the interac-

tion between Ce  $4f$  electrons should be mediated by the hybridization between Ce  $4f$  electrons and conduction electrons, mainly with Sn  $5p$  or Ni  $3d$  electrons. Further the Ce  $4f$ /Sn  $5p$  hybridization seems to be the major origin of the near- $E_F$  peak "A" in the Ce  $4f$  PSW because the intensity of the peak "A" is comparable to that of the peak "B", whereas in the Ni  $3d$  PSW the main Ni  $3d$  peak (at 1.4 eV in BE) is much stronger than the peak near  $E_F$ .

Note that the peak "B" exists in the  $4f$  derived PSW of CeNiSn, in addition to the well-known two peak structures, which indicates a good quality of data in this study. The location of the peak "B" is very close to that of the Ni  $3d$  main peak, suggesting that it originates from the hybridization of the Ni  $3d$  electrons with the Ce  $4f$  or  $5d$  electrons. This interpretation is consistent with the fact that no feature like "B" has been observed in the Ce  $4f$  PSW of CeSn<sub>3</sub> [26] which reveals only two peaks, corresponding to "A" and "C" above, respectively. Interestingly, the three peak structures in the difference spectrum of CeNiSn (Fig. 2) are very similar to those of CeBe<sub>13</sub> [21]. In the case of CeBe<sub>13</sub>, the Be  $s/p$  PSW has two peaks near  $E_F$  and at about 1.5 eV in BE, with the latter located around the middle peak in the difference spectrum. This middle peak in CeBe<sub>13</sub> has been assigned mainly due to Ce  $5d$  contribution. Further, the Ce  $5d$  wave functions have a larger overlap with the Ni  $3d$  wave functions than the Ce  $4f$  wave functions both in space and energy, and so the Ce  $5d$ /Ni  $3d$  hybridization would have a stronger contribution to the peak "B" than the Ce  $4f$ /Ni  $3d$  hybridization. Therefore it is likely that the feature "B" in CeNiSn has a substantial contribution from the Ce  $5d$  PSW (probably 30-50 %).

Figure 3 shows the yield spectra taken in the constant-final-state (CFS) and constant-initial-state (CIS) modes across the  $4d \rightarrow 4f$  threshold. The spectra have been scaled to have the same magnitude at the peak.  $E_i$  values in the CIS spectra denote initial state energies. The well-known Fano-like resonance in the Ce  $4f$  cross section is clearly observed in this figure. The line shapes of the Ce  $4f$  CIS and CFS yield spectra in CeNiSn are very similar to those of Ce metal [27], for which the Ce valence is close to  $3+$ . Moreover, the line shape of the Ce  $4f$  CIS in CeNiSn is essentially the same for different values of  $E_i$  over the Ce  $4f$  PSW, indicating that the  $4f$  emission does not have separate contributions from different valence states. However, drawing a quantitative conclusion on the valence of Ce in CeNiSn requires a detailed theoretical analysis of the  $4f$  CIS [28-30].

A finite metallic density of states has been observed at  $E_F$  above  $T_g$  in CeNiSn [31] (measured temperature  $T_{msr} \approx 20$  K  $>$   $T_g \approx 6$  K), suggesting that CeNiSn is likely to be metallic in the ground state or that the gap is anisotropic. To be consistent with the recent report of the metallic ground state, this feature of a finite density of states at  $E_F$  should persist even below  $T_g$ . To investigate the anisotropic electronic

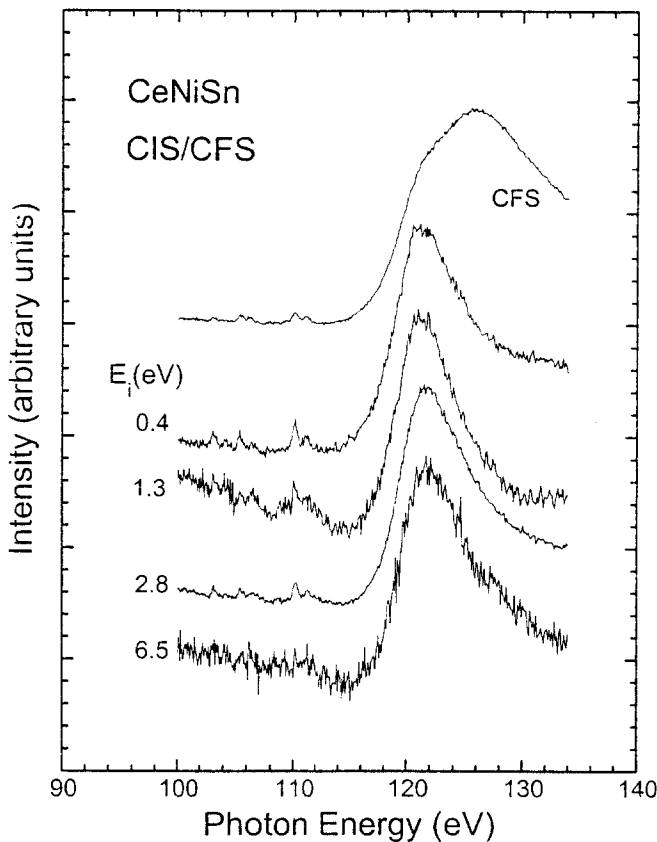


Fig. 3. Constant-initial-state (CIS) yield spectra of CeNiSn taken at initial state energies  $E_i$  of  $E_i=0.4$ , 1.3, 2.8, and 6.5 eV in BE's, respectively. A constant-final-state (CFS) yield spectrum taken at the kinetic energy  $E_k$  of 2 eV is also shown.

structure of CeNiSn more rigorously, it is required to perform ARPES measurements along different symmetry directions and to determine experimental band structures from the data.

#### 4. Conclusions

The electronic structure of the Kondo insulator CeNiSn has been investigated using photoemission spectroscopy (PES). The extracted Ce  $4f$  PSW exhibits three peak structures, including the well-known double-peak structures and a new peak located at the position of the Ni  $3d$  main peak. The peak near  $E_f$  in the two peak structures seems to reflect mainly the Ce  $4f$ /Sn  $5p$  or Ce  $4f$ /Ce  $5d$  hybridization, whereas an extra structure located around the Ni  $3d$  main peak reflects the Ce  $4f$ /Ni  $3d$  or Ce  $5d$ /Ni  $3d$  hybridization. In the valence band spectrum taken at the Ni  $3p \rightarrow 3d$  on-resonance energy, a satellite feature is observed about 6 eV below the Ni  $3d$  main peak, indicating a strong Ni  $3d$  Coulomb correlation. CIS and CFS yield spectra across the  $4d \rightarrow 4f$  threshold with several initial states over the Ce  $4f$  PSW are found to be very similar to those of Ce metal, indicating that the Ce valence is close to  $3+$ . The Fermi edge spectra also indicates a finite metallic density of

states at  $E_f$  above  $T_g$ .

#### Acknowledgments

We thank S. K. Kwon for his assistance in experiments. The authors wish to acknowledge the financial support of the Korea Research Foundation made in the program year of 1997, and that of the Korea Science and Engineering Foundation (KOSEF). The Synchrotron Radiation Center is supported by the National Science Foundation (NSF) under Grant No. DMR-95-31009.

#### References

- [1] T. Takabatake, Y. Nakazawa, and M. Ishikawa, Jpn. J. Appl. Phys. Suppl. **26**, 547 (1987).
- [2] T. Takabatake, M. Nagasawa, H. Fujii, G. Kido, M. Nohara, S. Nishigori, T. Suzuki, T. Fujita, R. Helfrich, U. Ahlheim, K. Fraas, C. Geibel, and F. Steglich, Phys. Rev. B **45**, 5740 (1992).
- [3] J. L. C. Daams and K. H. J. Buschow, Phillips J. Res. **39**, 77 (1984).
- [4] I. Higashi, K. Kobayashi, T. Takabatake, and M. Kasaya, J. Alloys and Compounds Res. **193**, 300 (1993).
- [5] Y. Inada, H. Azuma, R. Settai, D. Aoki, Y. Onuki, K. Kobayashi, T. Takabatake, G. Nakamoto, H. Fujii, and K. Maezawa, J. Phys. Soc. Jpn. **65**, 1158 (1996).
- [6] Y. Kagan, K. A. Kikon, and A. S. Mishchenko, Phys. Rev. B **55**, 12348 (1997).
- [7] T. Ekino, T. Takabatake, H. Tanaka, and H. Fujii, Phys. Rev. Lett. **75**, 4262 (1995).
- [8] T. Kasuya, Jpn. J. Appl. Phys. **8**, 3 (1993).
- [9] K. Ueda, H. Tsunetsugu, and M. Sigrist, Phys. Rev. Lett. **68**, 1030 (1992).
- [10] H. Ikeda and K. Miyake, J. Phys. Soc. Jpn. **65**, 1769 (1996).
- [11] M. Kyogaku, Y. Kitaoka, H. Nakamura, K. Asayama, T. Takabatake, F. Tshima, and H. Fujii, Physica B **171**, 235 (1991).
- [12] T. J. Sato, H. Kadowaki, H. Yashizawa, T. Ekino, T. Takabatake, H. Fujii, L. P. Regnault and Y. Isikawa, J. Phys. : Condens. Matter **7**, 8009 (1995).
- [13] G. Nakamoto, T. Takabatake, H. Fujii, A. Minami, K. Maezawa, I. Oguro, and A. A. Menovsky, J. Phys. Soc. Jpn. **64**, 4834 (1995).
- [14] A. Yanase and H. Harima, Prog. Theor. Phys. Suppl. **108**, 19 (1992).
- [15] T. J. Hammond, G. A. Gehring, M. B. Suvasini, and W. M. Temmerman, Phys. Rev. B **51**, 2994 (1995).
- [16] S. Nohara, H. Namatame, A. Fujimori, and T. Takabatake, Phys. Rev. B **47**, 1754 (1993); Physica B **186-188**, 403 (1993).
- [17] J. H. Scofield, J. Electron Spectrosc. Rel. Phenom. **8**, 129

- (1976); J. J. Yeh and I. Lindau, *Atom. Data Nucl. Data Tables* **32**, 1 (1985).
- [18] J. W. Allen, S. -J. Oh, O. Gunnarsson, K. Schönhammer, M. B. Maple, M. S. Torikachvili, and I. Lindau, *Adv. Phys.* **35**, 275 (1987).
- [19] S. Hüfner and G. K. Wertheim, *Phys. Lett.* **51A**, 299 (1975); *ibid* **51A**, 301 (1975).
- [20] B. I. Min, unpublished data.
- [21] J. M. Lawrence, J. J. Joyce, A. J. Arko, R. J. Barlett, P. C. Canfield, and Z. Fisk, *Phys. Rev. B* **47**, 15460 (1993).
- [22] The problem of separating out the Ce *4f surface* emission from the *4f bulk* emission remains. Qualitatively, the *surface 4f* emission is expected to be under the structure "C", as in other Ce compounds. See E. Weschke *et al.*, *Phys. Rev. Lett.* **69**, 1792 (1992).
- [23] O. Gunnarsson and K. Schönhammer, *Phys. Rev. B* **31**, 4815 (1985).
- [24] B. I. Min, H. J. F. Jansen, T. Oguchi, and A. J. Freeman, *Phys. Rev. B* **33**, 8005 (1986).
- [25] J. -S. Kang, K. C. Kang, and B. I. Min *Physica B* **230-232**, 497 (1997).
- [26] H. -D. Kim, O. Tjernberg, G. Chiaia, H. Kumigashra, T. Takahashi, L. Duo, O. Sakai, M. Kasaya, and I. Lindau, *Phys. Rev. B* **56**, 1620 (1997).
- [27] F. Gerken, A. S. Flodstrom, J. Barth, L. I. Johansson, and C. Kunz, *Phys. Scr.* **32**, 43 (1985).
- [28] D. W. Lynch and R. D. Cowan, *Phys. Rev. B* **36**, 9228 (1987).
- [29] O. Gunnarsson and T. C. Li, *Phys. Rev. B* **36**, 9488 (1987).
- [30] L. Braicovich, C. Carbone, O. Gunnarsson, and G. L. Olcese, *Phys. Rev. B* **44**, 13756 (1991).
- [31] J. -S. Kang *et al.*, unpublished data.